# Superradiance Transition in Photosynthetic Light-Harvesting Complexes

G.L.Celardo[1], F.Borgonovi,[1] M. Merkli,[2] V.I. Tsifrinovich,[3] and G.P. Berman[4]

[1]*Dipartimento di Matematica e Fisica and Interdisciplinary Laboratories for Advanced Materials Physics,*
*Università Cattolica, via Musei 41, 25121 Brescia, Italy and I.N.F.N., Sezione di Pavia, Italy*
[2]*Department of Mathematics and Statistics, Memorial University*
*of Newfoundland, St. John's, Newfoundland, Canada A1C 5S7.*
[3]*Department of Applied Physics, Polytechnic Institute of NYU,*
*6 MetroTech Center, Brooklyn, NY 11201, USA*
[4]*Theoretical Division, MS B213, Los Alamos National Laboratory, Los Alamos, NM 87545, USA*

(Dated: November 28, 2011)

We investigate the role of long-lasting quantum coherence in the efficiency of energy transport at room temperature in Fenna-Matthews-Olson photosynthetic complexes. The dissipation due to the coupling of the complex to a reaction center is analyzed using an effective non-Hermitian Hamiltonian. We show that, as the coupling to the reaction center is varied, the maximum efficiency in energy transport is achieved at the superradiance transition, characterized by a segregation of the imaginary parts of the eigenvalues of the effective non-Hermitian Hamiltonian. This approach allows one to study various couplings to the reaction center. We show that the maximal efficiency at room temperature is sensitive to the coupling of the system to the reaction center.

*Introduction.* The annual amount of energy humans currently use is delivered to Earth by the Sun in a few hours! Since solar energy is very dilute, it is essential to transport the captured energy efficiently. Most natural photosynthetic systems consist of antenna complexes, which capture photons from the Sun and transport energy to a reaction center (RC). There it is transformed into chemical energy via charge separation. Antenna complexes are able to transfer excitations to RCs with an efficiency exceeding 95%. For a long time, it was thought that energy transfer in photosynthetic light-harvesting complexes occurs through classical processes, similar to random walks of the excited electron to the RC. However, surprising evidence of coherent quantum energy transfer has been found recently [1, 2]. These findings raise two basic questions. How can coherence be maintained in complex biological systems at room temperature? Why is quantum coherence relevant to the efficiency of energy transfer?

The first question has been addressed in [3, 4]. We consider here the second one. It is known that quantum coherence can speed up energy transport through a quantum walk, which is faster than a classical walk [5]. It has been also pointed out in [6, 7] that a mechanism similar to Dicke superradiance [8], can enhance energy transport efficiency. We focus here on a different "superradiance transition" (ST) [9, 10], caused by quantum coherence and we show that ST can be employed to increase energy transport efficiency. To explain the ST, consider a discrete quantum system coupled to an environment having a continuum of states. The system-environment coupling alters the unperturbed energy levels: it causes an energy (Lamb) shift and the appearance of a resonance width (inverse of life-time). For weak coupling strength, the resonance widths are roughly the same. However, if the coupling strength reaches a critical value, at which

the resonance widths start to overlap, then a segregation of widths builds up. In this regime, almost the entire (summed up) decay width is allocated to just a few short-lived "superradiant states", while all other states are long-lived (and effectively decoupled from the environment). We call this segregation the "Superradiance Transition". This effect has been studied using random matrix theory [11, 12], in nuclear physics [13], for microwave billiards [14] and in paradigmatic models of coherent quantum transport [15, 16]. It was shown in [15] that in a realistic model for quantum transport, maximum transmission is achieved at ST.

In this Letter, we focus on transport properties of the Fenna-Matthews-Olson (FMO) complex, found in green sulphur bacteria. This complex, one of the most studied in the literature, acts as a conductor for energy transport between an antenna system and the RC. The FMO complex is a dissipative open quantum system. Here we take an effective non-Hermitian Hamiltonian approach [9, 10, 17] and study ST as a function of the coupling to the RC.

It has been shown recently that maximal transport efficiency for the FMO complex is achieved near a critical coupling to the RC [18]. However, so far, the value at which the maximum occurs, have not been determined. We compute this value analytically and we show that it is the value at which ST occurs. We also demonstrate that this effect is of pure quantum nature and cannot be described using a classical approach. We investigate different RC coupling schemes and show that the energy transport efficiency is sensitive to the coupling scheme.

*The Model.* The FMO complex is a trimer, composed of identical subunits, each of which contains seven bacteriochlorophylls (BChl). Each subunit acts independently

and can be modelled using a tight-binding Hamiltonian,

$$H_0 = \sum_{i=1}^{7} E_i |i\rangle\langle i| + \sum_{i,j} (J_{i,j}|i\rangle\langle j| + h.c.). \quad (1)$$

Here, $|i\rangle$ is the state in which site $i$ is excited and all other sites are in the ground state. Since the solar energy is very dilute, we limit the description to a single excitation in the complex, as is commonly done in the literature. We take the numerical values of $E_i$ and $J_{i,j}$ from [3].
The incident photon creates an electron-hole pair, called an exciton, which decays due to two processes: coupling with the photon bath (recombination) with associated decay time $T_1$, and coupling to the RC with decay time $T_{1r}$.
As is common in quantum optics [19], we describe the dissipative system with at most one excitation by states

$$|\psi\rangle = \sum_{i=1,7} a_i |0\rangle \otimes |i\rangle + \sum_c \int dE\, b_c(E) |c, E\rangle \otimes |gs\rangle, \quad (2)$$

where $|0\rangle$ is the vacuum state of the environments and $|c, E\rangle \otimes |gs\rangle$ is the state with one excitation in the environments and none on the sites. Here, $c$ is the quantum number labelling channels (at energies $E$) in the environments. The reduced density matrix is obtained by tracing over the states $|0\rangle$ and $|c, E\rangle$,

$$\rho = \sum_{i,j} a_i a_j^* |i\rangle\langle j| + (1 - \sum_i |a_i|^2)|gs\rangle\langle gs|, \quad (3)$$

which is of size $8 \times 8$. However, $\langle gs|\rho|i\rangle = 0$ since by (2), we neglect any transitions $|i\rangle \to |gs\rangle$. Moreover, $\langle gs|\rho|gs\rangle$ is just the loss of probability of excitation of the seven sites. Therefore, we restrict our considerations to the $7 \times 7$ matrix $\langle i|\rho|j\rangle$, $1 \le i, j \le 7$, which however does not have constant trace.
In order to compute the evolution of the reduced density matrix we introduce an effective non-Hermitian Hamiltonian [9, 15, 20] which in general can be written as, $H_{\text{eff}}(E) = H_0 + \Delta(E) - iW(E)$, where $H_0$ is the Hermitian Hamiltonian of the system decoupled from the environments and $\Delta(E)$ and $W(E)$ are the induced energy shift and the dissipation, respectively. Neglecting the energy dependence and the energy shift we have $H_{\text{eff}} = H_0 - iW$. The real symmetric matrix $W$ is given by the bound state-continuum transition amplitudes, $W_{ij} = \sum_c A_i^c (A_j^c)^*$, where $A_i^c$ is the transition amplitude from state $i$ to channel $c$.
The coefficients $a_i$ in Eq. (3) satisfy

$$i\hbar \dot{a}_j = \sum_{k=1}^{7} \left\{ H_{0jk} a_k - iW_{jk} a_k \right\} \quad (4)$$

and so we obtain

$$i\hbar \dot{\rho}_{jk} = [H_0, \rho]_{jk} - i \sum_{l=1}^{7} \left\{ W_{jl}\rho_{lk} + \rho_{jl}W_{lk} \right\}. \quad (5)$$

Under the standard assumption [21, 22] that each site is coupled to an independent (local) environment, with associated coupling time $T_1$, we have $A_i^i = \sqrt{\hbar/2T_1}$, $i = 1, .., 7$. The site $i = 3$ is the only one which is, in addition, coupled to the RC, giving rise to a decay time $T_{1r}$. Then $A_3^8 = \sqrt{\hbar/2T_{1r}}$ (in this scheme there are 7+1 channels); all the other $A_i^c = 0$. Let us notice that the interactions with the environments and the RC are encoded entirely by relaxation parameters $T_1$ and $T_{1r}$.
Within this formalism it is very easy to consider different coupling schemes, e.g., when the $k$-th site is also coupled to the same channel in RC, then one simply puts $A_k^8 = \sqrt{\hbar/2T_{1r}}$.
One can verify that equation (5) can also be obtained by restriction to the $7 \times 7$ density matrix, from a Lindblad dynamics for the full $8 \times 8$ density matrix (3).
In the following, we fix $T_1 = 1$ns, which is the reorganization time reported in the literature, and we focus on the effect of varying $T_{1r}$.
*Superradiance transition.* ST can be analyzed by studying the complex eigenvalues $\mathcal{E}_r = E_r - i\Gamma_r/2$ of $H_{\text{eff}}$. As the coupling between the excitonic states and the RC increases, one observes a rearrangement of the widths $\Gamma_r$ (the "superradiance" transition [15]). We show this effect in Fig. 1 (left panel), where the largest width (red dashed curve) and the average of the $7 - 1 = 6$ smallest widths (black full curve) are plotted as functions of $T_{1r}$. For weak coupling to RC (large $T_{1r}$) the widths of all states increases as $T_{1r}$ decreases. On the other hand, below a critical value $T_{1r}^{cr}$, corresponding to ST, (green full line), the average of the 6 smallest widths decreases while the largest width, corresponding to the superradiant state, increases. To examine localization of the excitation we use the Inverse Participation Ratio (IPR) of a state $|\psi\rangle$, defined as $(\sum_i |\langle i|\psi\rangle|^4)^{-1}$. Its value varies from 1 for fully localized to 7 for fully delocalized states. The right panel of Fig. 1 shows the IPR for the state associated to the largest width (the one decaying most quickly). In the superradiant regime, $T_{1r} < T_{1r}^{cr}$, this state is fully localized on site 3, the only site connected to the RC. For weak coupling to the RC, $T_{1r} > T_{1r}^{cr}$, the IPR is approximately 1.6. This small value, as compared to the maximal possible value of 7, is explained by (Anderson) localization [23] of the eigenstates on sites. The critical value $T_{1r}^{cr}$, at which ST occurs, can be estimated analytically. If all the states have roughly the same width, at least for small coupling, then the superradiance condition coincides with that of overlapping resonances. This reasoning can be adapted to the FMO system. Here, eigenstates are mostly localized on the sites, and only site 3 is coupled to the RC. The widths are thus not uniform and most of the total width belongs to the eigenstate localized at site 3. Imposing that the half width $\Gamma_3/2$ is approximately equal to the mean level spacing $D$, $\Gamma_3/2 \approx D$ and using that $\Gamma_3 \approx \hbar/T_{1r}$, we obtain the critical value at which ST occurs, $T_{1r}^{cr} \approx \hbar/2D$. In the FMO system, the energy level spacing is $D/hc \approx 83.5\ cm^{-1}$, which gives $T_{1r}^{cr} \approx 0.03$ ps, a value in very good agreement with the numerical results of Fig. 1 (vertical line).
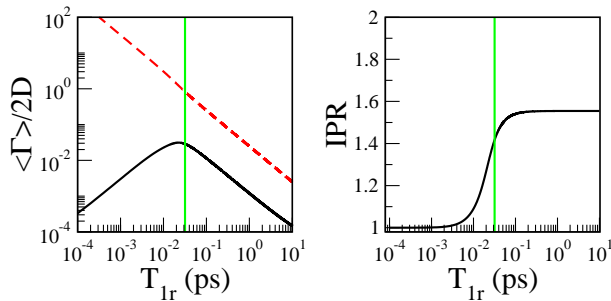*Efficiency of energy transport.* Interactions with the

FIG. 1: (Color online) Left panel : average decay width, normalized to the mean level spacing, $D$ as a function of the coupling time to the RC, $T_{1r}$. The black curve represents the average decay width of the 6 states with smallest width, while the dashed red curve shows the largest decay width. Right panel : IPR of the eigenstate of $H_{\text{eff}}$ with the largest width as a function of $T_{1r}$. In both panels the vertical green line indicates the critical value of $T_{1r}$ at which ST occurs.

surrounding phonon environment is taken into account by adding to the Hamiltonian a fluctuating diagonal term, which induces pure dephasing without dissipation, as in [21]: $H_{SB} = \sum q_i(t)|i\rangle\langle i|$ , with $\langle q_i(t)q_j(t)\rangle = \hbar^2 c\delta_{i,j}\delta(t)\gamma_\phi$. The associated dephasing time is $T_d = 1/c\gamma_\phi$ . We take into account this term in our numerical simulations by adding a dephasing Lindblad operator to the master equation (5), as was done in Ref. [19]. We use the experimental value $\gamma_\phi = 0.52\,T\,cm^{-1}/K$ [2], where $T$ is the temperature in Kelvin.

Transport efficiency has been measured by the probability that the excitation is in the RC at time $t_{max}$ [22],

$$\eta(t_{max}) = (1/T_{1r})\int_0^{t_{max}} dt\,\rho_{33}(t), \qquad (6)$$

and by the average transfer time to the RC [21],

$$\tau = (1/T_{1r})\int_0^\infty dt\,t\,\rho_{33}(t)/\eta(\infty). \qquad (7)$$

In our simulations, we take the initial state $\rho(0) = (1/2)(|1\rangle\langle 1| + |6\rangle\langle 6|)$, since sites 1 and 6 receive the excitation from the antenna system [21].

It was numerically found in [18] that efficiency reaches a maximum as a function of $T_{1r}$. Here, we explain it as a consequence of ST, a general phenomenon in coherent quantum transport. In Fig. 2, we plot $\eta(t_{max} = 5\,ps)$ (left panel), and $\tau$ (right panel), as functions of $T_{1r}$. The maximum efficiency of energy transport (maximum $\eta$ and minimum $\tau$) is reached near the ST (vertical line). Note that $\eta(t_{max} = 5\,ps)$ has a maximum not only in the quantum limit ($T = 0.1\,K$, black dashed curve), but also at room temperature ($T = 300\,K$, red thick curve), so ST persists also in presence of dephasing. Within the frame of ST, the decrease of efficiency for large coupling to RC, can be interpreted as a localization effect, see Fig. 1 (right panel). Our results also show that dephasing can increase efficiency due to coherence, since it counteracts quantum localization. This effect is known as Environment-

Assisted Quantum Transport (ENAQT) [21, 22]. The transfer time has a minimum near the ST of the order of a few picoseconds. This time is comparable with the transfer times estimated in the literature. The coupling
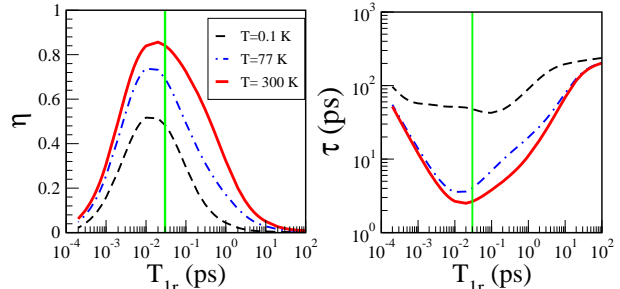


FIG. 2: (Color online) Left panel : efficiency computed at $t_{max} = 5$ ps, see Eq. (6), as a function of $T_{1r}$, for different temperatures. Right panel: average transfer time, see Eq. (7), as a function of $T_{1r}$, for the same temperatures. ST has been indicated as a green vertical line. The initial condition is $\rho(0) = (1/2)(|1\rangle\langle 1| + |6\rangle\langle 6|)$.

to the RC also induces a shift of the energy of site 3 (not only a decay width) [15]. This shift is generically of the form $\delta = \epsilon/T_{1r}$, where $\epsilon$ depends on the details of the coupling. We checked that the effect of changing $\epsilon$ randomly, so as to produce a 50 % change in the average level spacing, merely changes the efficiency by a few percent.

*Quantum vs. classical.* ST implies the presence of a maximum of the energy transport efficiency as a function of the coupling time to the RC. This effect is counter-intuitive from a classical point of view. Indeed, the probability to escape (decay) for a classical particle does not decrease as the escape rate (from site 3) is increased. In order to show the role of quantum coherence, consider a classical master equation for the population dynamics, as in the Forster approach [24]:

$$dP_i/dt = \sum_k T_{i,k}P_k - P_i/T_1 - \delta_{i,3}P_i/T_{1r}, \qquad (8)$$

where $P_i$ is the probability to be on site $i$, $T_{i,k}$ is the transition matrix and the last two terms take into account the possibility for the classical excitation to escape the system. The transition rates from site $i$ to site $k$ have been computed from [25], neglecting the dependence on the coupling to the RC (for a classical particle, the probability to go from any site to site 3 does not depend on the coupling to the RC). The comparison between the classical and quantum behavior is shown in Fig. 3 (left panel). The classical dynamics leads to a very different dependence of the efficiency on $T_{1r}$, it does not exhibit a maximum but simply decays with $T_{1r}$. This shows that the ST effect is due to quantum coherence.

*Different coupling schemes.* So far, we have considered the site 3 to be the only one coupled to the RC. How-
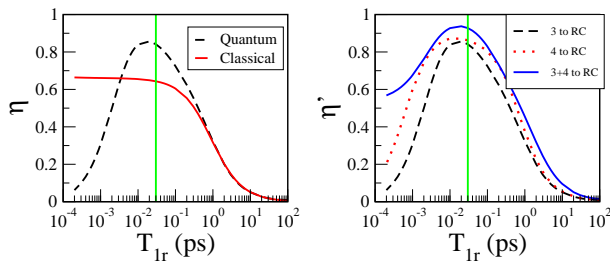
FIG. 3: (Color online) Left panel : quantum and classical efficiency computed at $t_{max} = 5$ ps, as a function of $T_{1r}$ at room temperature $300\,K$. Right panel : efficiency computed at $t_{max} = 5$ ps, using Eq. (9), as a function of $T_{1r}$, for different coupling to RC. The vertical green line represents ST. As initial conditions we choose $\rho(0) = (1/2)(|1\rangle\langle 1| + |6\rangle\langle 6|)$.

ever, it is not known for sure which site(s) connect to the RC, even though sites 3 and 4 are the most likely candidates, since they are closest to it [21]. As mentioned above, the non-Hermitian Hamiltonian formalism easily allows to describe different coupling schemes. We compare the efficiency in the following three situations: only site 3 is coupled to RC (as done above), only site 4 is coupled to the RC, both sites 3 and 4 are coupled to the RC. In a general setting the probability for the excitation to be in the RC at time $t_{max}$ cannot be computed using Eq. (6), since by merely summing that expression for each site connected to the RC, we neglect interference effects. The efficiency should be computed as

$$\eta'(t_{max}) = 1 - Tr(\rho(t_{max})) - \frac{1}{T_1}\int_0^{t_{max}} dt\, Tr(\rho(t)). \quad (9)$$

Here, $1 - Tr(\rho(t_{max}))$ is the probability that the excitation leaves the system by the time $t_{max}$. The last term in Eq. (9) is the probability that the excitation has been lost by recombination during this time. If there is just one decay channel, then Eq. (9) reduces to Eq. (6).

In Fig. 3 (right panel) we show that the efficiency is sensitive to different coupling schemes. In particular, we notice that coupling through site 4 achieves higher efficiency than through site 3. If both sites are coupled to the RC, then the efficiency is further improved, and its decay for small coupling times is smaller than that for a single coupled site.

*Conclusion.* We have analyzed energy transport in the FMO system. We have shown that with decreasing strength of the coupling to the reaction center, a superradiance transition occurs. This transition happens at the same critical value of the coupling for which energy transport efficiency is maximal. We have estimated this critical value analytically. We have also given a general scheme for different couplings (several sites coupled to the reaction center). For coupling strength close to the critical one, where the superradiance transition takes place, we obtain energy transfer times comparable to experimental values (a few picoseconds). Our results show that the superradiance mechanism might play an important role in explaining the efficiency of quantum transport in photosynthetic light-harvesting systems.

[1] G.S. Engel et al., Nature **446**, 782 (2007).

[2] G. Panitchayangkoon et al., PNAS **107**, 12766 (2010).

[3] M. Sarovar, A. Ishizaki, G.R.Fleming and K.B.Whaley, Nature Physics **6**, 462 (2010).

[4] H. Hossein-Nejad1 and G. D. Scholes, New J. Phys. **12**, 065045 (2010).

[5] M. Mohseni, P. Rebentrost, S. Lloyd and A. Aspuru-Guzik, J. Chem. Phys. **129**, 174106 (2008).

[6] S. Lloyd and M. Mohseni, New J. Phys. **12**, 075020 (2010).

[7] G. D. Scholes, Chem. Phys. **275**, 373 (2002).

[8] R. H. Dicke, Phys. Rev. **93**, 99 (1954).

[9] V. V. Sokolov and V. G. Zelevinsky, Nucl. Phys. **A504**, 562 (1989); Phys. Lett. B **202**, 10 (1988); I. Rotter, Rep. Prog. Phys. **54**, 635 (1991).

[10] V. V. Sokolov and V. G. Zelevinsky, Ann. Phys. (N.Y.) **216**, 323 (1992).

[11] J. J. M. Verbaarschot, H. A. Weidenmüller, and M. R. Zirnbauer, Phys. Rep. **129**, 367 (1985); N. Lehmann, D. Saher, V. V. Sokolov, and H.-J. Sommers, Nucl. Phys. **A582**, 223 (1995); Y. V. Fyodorov and H.-J. Sommers, J. Math. Phys. **38**, 1918 (1997); H.-J. Sommers, Y. V. Fyodorov, and M. Titov, J. Phys. A: Math. Gen. **32**, L77 (1999).

[12] G. L. Celardo, F. M. Izrailev, V. G. Zelevinsky, and G. P. Berman, Phys. Lett B **659**, 170 (2008); G. L. Celardo, F. M. Izrailev, V. G. Zelevinsky, and G. P. Berman, Phys. Rev. E, **76**, 031119 (2007); G. L. Celardo, S. Sorathia, F. M. Izrailev, V. G. Zelevinsky, and G. P. Berman, CP995, Nuclei and Mesoscopic Physics - WNMP 2007, ed. P. Danielewicz, P. Piecuch, and V. Zelevinsky.

[13] A. Volya and V. Zelevinsky, Phys. Rev. C **67**, 054322 (2003); Phys. Rev. Lett. **94**, 052501 (2005); Phys. Rev. C **74**, 064314 (2006).

[14] H.-J. Stöckmann, E. Persson, Y.-H. Kim, M. Barth, U. Kuhl, and I. Rotter, Phys. Rev. E **65**, 066211 (2002); R. G. Nazmitdinov, H.-S. Sim, H. Schomerus, and I. Rotter, Phys. Rev. B **66**, 241302 (2002).

[15] G.L. Celardo and L. Kaplan, Phys. Rev. B **79**, 155108 (2009); G. L. Celardo, A. M. Smith, S. Sorathia, V. G. Zelevinsky, R. A. Senkov, and L. Kaplan, Phys. Rev. B **82**, 165437 (2010).

[16] A. F. Sadreev and I. Rotter, J. Phys. A **36**, 11413 (2003).

[17] C. Mahaux and H. A. Weidenmüller, *Shell Model Approach to Nuclear Reactions* (North Holland, Amsterdam, 1969).

[18] M. Mohseni, A. Shabani, S. Lloyd, H. Rabitz, arXiv:1104.4812v1 [quant-ph]; A. Shabani, M. Mohseni, H. Rabitz, S. Lloyd, arXiv:1103.3823v3 [quant-ph].

[19] P.W. Milonni and P.L. Knight, Phys. Rev. A **10**, 1096 (2009).

[20] A. Messiah, *Quantum Mechanics* (North Holland Publishing company, Amsterdam 1962) English ed. Vol II, Chapter $XXI$.13.

[21] P. Rebentrost, M. Mohseni, I.Kassal, S. Lloyd and A. Aspuru-Guzik, New J. Phys. **11**, 033003 (2009); P. Rebentrost, M. Mohseni and A. Aspuru-Guzik A, J. Phys. Chem. B **113**, 9942 (2009).

[22] M. B. Plenio and S. F. Huelga, New J. Phys. **10**, 113019 (2008); F. Caruso, A. W. Chin, A. Datta, S. F. Huelga and M. B. Plenio, J. Chem. Phys. **131**, 105106 (2009).

[23] P. W. Anderson, Phys. Rev. **109**, 1492 (1958).

[24] Th. Forster, In *Modern Quantum Chemistry*, Sinannouglu, O., Ed.; Acad. Press: New York, (1965) p. 93.

[25] J.A. Leegwater, J. Phys. Chem. **100**, 14403 (1996).